

Cathodoluminescence (CL) behaviour and crystal chemistry of apatite from rare-metal deposits

U. KEMPE* AND J. GÖTZE

TU Bergakademie Freiberg, Institute of Mineralogy, Brennhausgasse 14, D-09596 Freiberg, Germany

ABSTRACT

Apatite samples from rare-metal mineralization were investigated by a combination of cathodoluminescence (CL) microscopy and spectroscopy, microchemical analysis and trace element analysis. Internal structures revealed by CL can be related to variations in the crystal chemistry and may sometimes reflect changes in the composition of the mineralizing fluids.

Apatite from mineralization related to alkaline rocks and carbonatites (Type 1) typically exhibits relatively homogeneous blue and lilac/violet CL colours due to activation by trace quantities of rare earth element ions (Ce^{3+} , Eu^{2+} , Sm^{3+} , Dy^{3+} and Nd^{3+}). These results correlate with determined trace element abundances, which show strong light rare earth element (*LREE*) enrichment for this type of apatite. However, a simple quantitative correlation between emission intensities of $\text{REE}^{3+/2+}$ and analysed element concentrations was not found.

Apatite from P-rich altered granites, greisens, pegmatites and veins from Sn-W deposits (Type 2) shows strong Mn^{2+} -activated yellow-greenish CL, partially with distinct oscillatory zoning. Variations in the intensity of the Mn^{2+} -activated CL emission can be related either to varying Mn/Fe ratios (quenching of Mn activated CL by Fe) or to self-quenching effects in zones with high Mn contents (>2.0 wt.%). The *REE* distribution patterns of apatite reflect the specific geological position of each sample and may serve as a "tracer" for the *REE* behaviour within the ore system. Although the *REE* contents are sometimes as high as several hundred parts per million, the spectral CL measurements do not exhibit typical *REE* emission lines because of dominance of the Mn emission. In these samples, *REE*-activated luminescence is only detectable by time-resolved laser-induced luminescence spectroscopy.

Both types of apatite (Type 1 in the core and Type 2 in the rim) were found in single crystals from the Be deposit Ermakovka (Transbaikalia). This finding proves the existence of two stages of mineralization within this deposit.

KEYWORDS: apatite, rare-metal deposits, cathodoluminescence, trace-elements, rare earth elements.

Introduction

APATITE (general formula $\text{Ca}_5[(\text{PO}_4)_3(\text{OH},\text{F},\text{Cl})]$) is an important accessory mineral in various types of igneous, sedimentary and metamorphic rocks. Due to chemical substitutions within the apatite lattice, the Ca^{2+} sites can be occupied by a number of cations, including but not limited to Sr^{2+} , Mn^{2+} , Fe^{2+} , rare earth elements ($\text{REE}^{2+/3+}$), Y^{3+} and Na^+ . The site preference of Mn^{2+} , Sr^{2+}

and REE^{3+} to either the ninefold Ca(1) or sevenfold Ca(2) sites in the apatite structure remains a point of controversy (e.g. Morozov *et al.*, 1970; Marfunin, 1979; Hughes *et al.*, 1991a,b; Gaft *et al.*, 1998). Ions such as Cl^- and OH^- can substitute for F^- in the apatite structure and P^{5+} can be partly replaced by Si^{4+} , As^{5+} , S^{6+} and C^{4+} (Elliot, 1994). Because of differences in the valence of the substituting ions, a coupled substitution is sometimes required to maintain charge balance, e.g. $2\text{Ca}^{2+} \leftrightarrow \text{Na}^+ + \text{REE}^{3+}$ or $\text{Ca}^{2+} + \text{P}^{5+} \leftrightarrow \text{REE}^{3+} + \text{Si}^{4+}$ (Rønsbo, 1989; Finch and Fletcher, 1992; Elliot, 1994; Coulson and Chambers, 1996; Rae *et al.*, 1996). Another

* E-mail: kempe@mineral.tu-freiberg.de

DOI: 10.1180/0026461026610019

mechanism for charge balancing, sometimes causing deviations from stoichiometric composition, is a substitution in the form of $3\text{Ca}^{2+} \leftrightarrow 2\text{REE}^{3+} + \square$ (where \square is a site vacancy, *cf.* Elliot, 1994).

It was previously observed that incorporation of trace elements in accessory apatite depends on the petrology and specifics of the host rocks (e.g. Zhang *et al.*, 1985; Fleischer and Altschuler, 1986; Boudreau and Kruger, 1990). Thus, geochemical features of apatite can be used as an important tool for mineralogical and geological interpretation (*cf.* Landa *et al.*, 1983; Fleischer and Altschuler, 1986; Wenzel and Ramseyer, 1992; Pan and Fleet, 1996; Rae *et al.*, 1996; Whitney and Olmsted, 1998; Irber, 1999; Perseil *et al.*, 2000; Seifert *et al.*, 2000).

Imaging of internal structures and alteration features in natural apatite by cathodoluminescence (CL) microscopy provides essential information on rock formation and mineralization processes, particularly fluid evolution (Knutson *et al.*, 1985; Finch, 1992; Wenzel and Ramseyer, 1992; Coulson and Chambers, 1996; Rae *et al.*, 1996; Perseil *et al.*, 2000). Apatites from different parent rocks or mineral parageneses were found to exhibit various CL and photoluminescence (PL) emissions. For example, apatite from granitic rocks and pegmatites typically exhibits yellowish to orange CL and PL, whereas apatite from carbonatites and other alkaline rocks tends to show blue, violet or lilac CL and PL (e.g. Portnov and Gorobets, 1969; Marfunin, 1979; Mariano, 1988). The characterization of luminescence colour alone, however, is of qualitative nature only and does not necessarily permit identification of all ions responsible for the luminescence colour. Spatially-resolved cathodoluminescence spectroscopy provides useful information about emission centres and their intra-crystal distribution (e.g. Rakovan and Reeder, 1996). In particular, Mn^{2+} and *REE* ions serve as effective activators in apatite. Investigations on synthetic and naturally occurring apatite have revealed characteristic emission bands (Mn^{2+} , Eu^{2+} , Ce^{3+}) or sets of emission peaks (*REE*³⁺ but not Ce^{3+}) that can be related to specific activator ions (e.g. Portnov and Gorobets, 1969; Kuznecov and Tarashchan, 1975; Marfunin, 1979; Roeder *et al.*, 1987; Mariano, 1988; Blanc *et al.*, 1995; Rakovan and Reeder, 1996; Mitchell *et al.*, 1997; Blanc *et al.*, 2000). Data concerning peak identification are summarized in Götze *et al.* (2001). On the other hand, as shown for synthetic

samples and As-rich natural apatite, the incorporation of Fe^{2+} or As^{5+} into the apatite structure can result in significant quenching of the luminescence intensity (Filippelli and Delaney, 1993; Perseil *et al.*, 2000).

Apatite is a common constituent in mineral assemblages from several types of ore deposits. In the present study, two types of occurrences are examined and discussed in detail: (1) apatite from mineralization in relation to alkaline rock sequences including carbonatites; and (2) apatite from P-rich altered granites, greisens, pegmatites and veins from Sn-W deposits. The purpose of the study is to reveal variations in chemical composition and related CL behaviour of apatite from these two settings. The verification of the prevailing CL activation and quenching mechanisms in the mineral was possible due to contrasting crystal chemistry of the samples investigated. Consequences for genetic interpretations based on CL investigations are discussed briefly in conclusion.

Geological setting, materials and methods

The sample locations are reported in Table 1. One sample from Kovdor (Kola Peninsula, Russia) and two samples from Mushugai Khudug (Gobi desert, Mongolia) represent apatite from carbonatite complexes. Apatite from larvikite from an open pit at Svensken (Norway) is included in our study representing the occurrence in alkaline rocks. Samples from Sn-W deposits derive from Ehrenfriedersdorf (Central Erzgebirge, Germany), Sadisdorf (Eastern Erzgebirge, Germany) and Vysoky Kamen (Slavkovsky les, Czech Republic; *cf.* Jachovsky, 1994; René, 1998).

The Kovdor massif consists of a sequence of ultrabasic-alkaline-carbonatite rocks (Kharlamov *et al.*, 1981). The sample investigated derives from the main magnetite-apatite ore body (Landa *et al.*, 1983). At Mushugai, the alkaline rocks are in general acidic. Mushugai apatite was sampled from a small magnetite-apatite ore body but near the contact with the surrounding syenite. The mineral occurs as idiomorphic crystals intergrown with phlogopite. More details of the mineralogy and geology of the Mushugai massif are presented in Baskina *et al.* (1978), Vasil'eva *et al.* (1978), Ontoev *et al.* (1979) and Rundqvist *et al.* (1995).

An apatite sample with distinct colour zonation (core – yellowish-green, rim – bluish green) was collected from a Be orebody in Ermakovka (Transbaikalia, Russia). Be-F orebodies are

TABLE 1. Apatite samples from different rare-metal deposits selected for the present study.

Sample	Lithology/location	Characteristic
KOV	carbonatite complex Kovdor, Kola Peninsula	white-green columnar crystal
MH 114	alkali complex, borehole 1 Mushugai khudug, Mongolia	yellowish-green short-prismatic crystals
SVEN	larvikite, Svensken, Norway	dark green prismatic crystal
YM	apatite ore Be-F metasomatite Ermakovka, Transbaikalia	fragments of zonal coloured crystals; core: yellowish-green; rim: bluish-green
A3	greisen in albite granite Vierung, Ehrenfriedersdorf, Germany	dark green crystal fragments
A4	apatite breccia in metasomatized granite Zypressenbaumer Gangzug, Ehrenfriedersdorf, Germany	light blue crystal fragments
A5	Greifenstein granite, 'Topasloch' Ehrenfriedersdorf, Germany	short-prismatic purple crystals
A6	apatite breccia Prinzler vein, 6th level, Ehrenfriedersdorf, Germany	partly zoned crystals and fragments; core: bluish, rim: white
A8	quartz vein, pinge, Sadisdorf, Germany	fragments of green crystals
A9	apatite breccia Prinzler West, 2. Gezeugstrecke, Ehrenfriedersdorf, Germany	dark bluish-green columnar crystal
A10	apatite in K-feldspar-pegmatite 5th level, Ehrenfriedersdorf, Germany	dark green crystals
VY101	altered topaz-bearing granite, open pit, Vysoky Kamen, Czech Republic	crystal intergrown with quartz and muscovite

developed as zones of metasomatic alteration within Upper Proterozoic schist, limestone and dolomite near their contact with Jurassic subalkaline granites (Novikova *et al.*, 1994; Lykhin *et al.*, 2001). The apatite was sampled from an altered dolomite near the largest ore body of the deposit, where it occurs in association with dolomite, phlogopite and fluorite.

Three samples (A4, A6 and A9) are from a breccia in the near exocontact of the Sauberg cupola of the Ehrenfriedersdorf Sn-W deposit (Central Erzgebirge, Germany). The breccia contains angular granite, apatite and schist fragments cemented by vein quartz (Fig. 1). Another sample derives from a pipe-like topaz-albite-granite body near the top of the granite cupola of the Greifenstein area (A3) and an additional one (A5) from cassiterite-bearing mica greisen from the upper part of the Vierung granite cupola. The geology and mineralogy of the Ehrenfriedersdorf deposit is described by Hösel (1994) and Seltmann *et al.* (1995).

Carbon-coated polished thin-sections of all samples were investigated by a combination of polarizing microscopy and CL microscopy and spectroscopy. The CL examinations were initially performed on a 'hot cathode' CL microscope at 14 kV and with a current density of $\sim 10 \mu\text{A}/\text{mm}^2$. Luminescence images were captured 'on-line' during CL operations by means of an adapted digital video-camera (KAPPA 961-1138 CF 20 DXC with cooling stage). The CL spectra were obtained using an EG&G digital triple-grating spectrograph with a liquid nitrogen-cooled, Si-based charge-coupled device (CCD) detector (Rieser *et al.*, 1994). The CCD camera was attached to the CL microscope by a silica-glass fibre guide. The CL spectra were measured in the range 380 to 1200 nm using standardized conditions (wavelength calibration by a Hg lamp). To prevent any falsification of the CL spectra due to electron bombardment, all spectra were taken on non-irradiated sample spots.

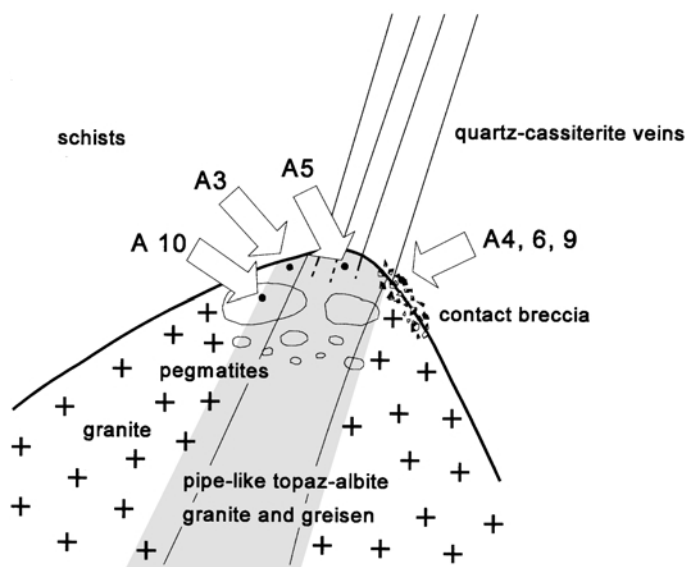


FIG. 1. Schematic sketch of sample locations in the Ehrenfriedersdorf Sn-W deposit (Central Erzgebirge, Germany). Apatite samples A4, A6, A9 are from a breccia in the near exocontact of the Sauberg cupola; sample A3 derives from a pipe-like topaz-albite-granite body near the top of a granite cupola in the Greifenstein area; sample A10 from a pegmatite body and sample A5 comes from a cassiterite-bearing mica greisen from the upper part of the Vierung granite cupola.

In addition, panchromatic and spectral CL investigations and energy dispersive X-ray analysis (EDX) were carried out using a JEOL JSM 6400 SEM. This SEM is equipped with an Oxford Instruments MonoCL system, an additional panchromatic CL detector, a BSE detector and a Noran/Vantage EDX system with a light element Si(Li) detector. For CL investigation, the accelerating voltage was set at 20 kV and the beam current in the range 0.6–1.6 nA. The CL spectra were detected over the range 200–800 nm, with 1 nm steps and a dwell time of 1 s per step. For EDX analyses, the microscope was operated at 20 kV and 0.6 nA. Detection limits were 0.1 wt.% for Fe, 0.2 wt.% for Mn, 0.2 wt.% for La and Ce, and 0.3 wt.% for Nd.

The combination of CL measurements on an optical CL microscope and a SEM enabled us: (1) to produce true CL colour images as well as high-resolution panchromatic SEM-CL images comparing them to BSE images; (2) to get spectral information from the UV (200 nm) up to the IR (1200 nm); and (3) to realise time-resolved spectral CL measurements of all samples.

Some of the samples were also measured by laser-induced time-resolved luminescence spec-

troscopy. Details of the method are reported elsewhere (Gaft *et al.*, 1998).

To obtain more information on the trace element composition of investigated apatite, separated aliquots of selected samples and differently coloured crystal zones, respectively, were investigated by inductively coupled plasma mass spectrometry (ICP-MS) analysis (see Table 2). Analyses were performed using a Perkin Elmer Sciex Elan 5000 quadrupole instrument with a cross-flow nebulizer and a rhyton spray chamber (see Monecke *et al.*, 2000a for more details of the analytical procedure).

Results and discussion

Apatite from mineralization in alkaline rocks and carbonatites

Samples from Kovdor, Mushugai and Svensken

The apatite from the carbonatite of Kovdor shows relatively homogeneous (unzoned) blue to lilac CL with inclusions of orange luminescing calcite (Fig. 2a) occasionally intergrown with richterite. Under CL this apatite behaves in a similar fashion to apatites from alkaline rocks reported from elsewhere (Portnov and Gorobets, 1969; Mariano, 1988; Finch, 1992; Coulson and

CL BEHAVIOUR AND CRYSTAL CHEMISTRY OF APATITE

TABLE 2. Trace-element concentrations (in ppm) in selected apatite samples from different ore deposits, detected by ICP-MS.

	Kovdor carbonatite white-green (KOV)	Ermakovka apatite ore		Ehrenfriedersdorf	
		yellow-green (YM) core	bluish-green (YM) rim	breccia white-bluish (A6)	granite violet (A5)
Al	104	269	249	140	287
Mg	613	99	120	108	29
Ba	30	321	205	2	3
Sr	2230	8160	29000	8210	9600
K	nn	118	53	92	119
Na	1509	2100	1300	198	71
Mn	101	870	13800	6930	4070
Fe	nn	849	1000	575	335
Pb	17	11	102	62	13
U	11	9	40	206	1
Th	1000	386	7230	77	11
Y	150	65	776	556	4.13
La	1674	5130	124	5.6	2.09
Ce	3770	6110	185	14.5	3.24
Pr	474	452	16	3.0	0.29
Nd	1740	887	46	16.4	0.76
Sm	230	91	10.5	10.9	0.25
Eu	55	19	2.6	11.1	0.06
Gd	181	65	10.1	16.2	0.27
Tb	19	9	2.2	5.5	0.07
Dy	55	30.4	17.1	52.5	0.41
Ho	7	4.5	4.6	12.9	0.06
Er	14	9.9	27.5	54.1	0.16
Tm	1	1.4	9.1	11.2	0.03
Yb	6	8.4	102	93.8	0.28
Lu	1	1.1	17	13.3	0.04

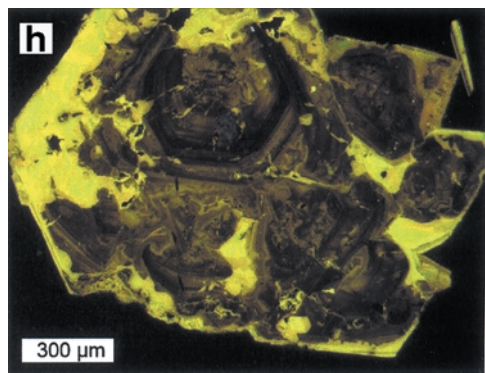
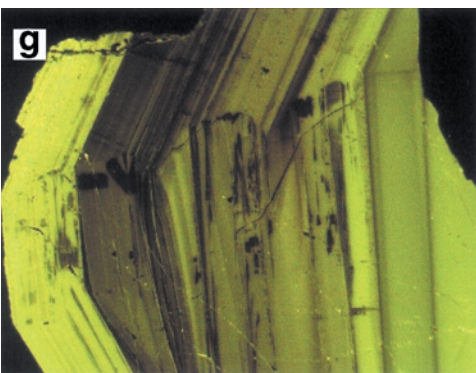
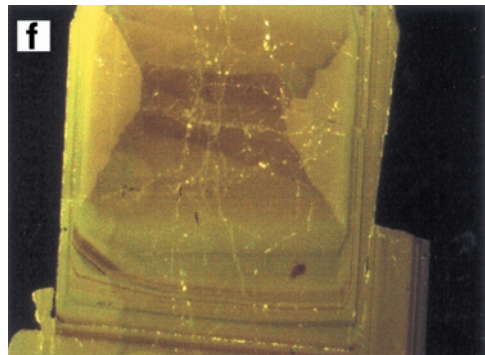
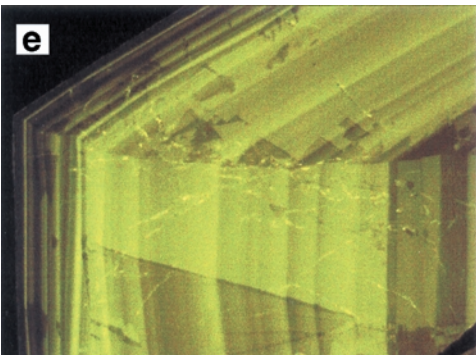
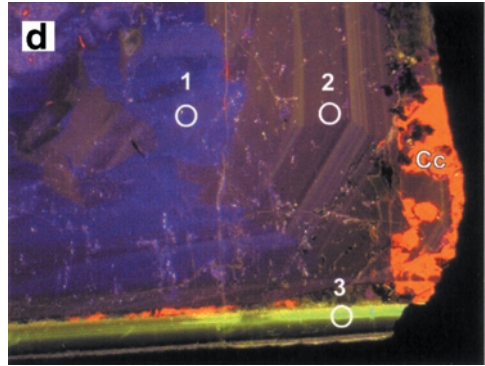
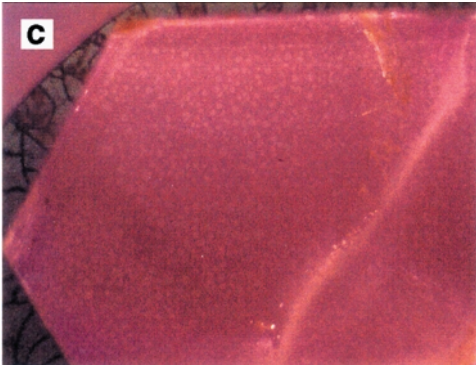
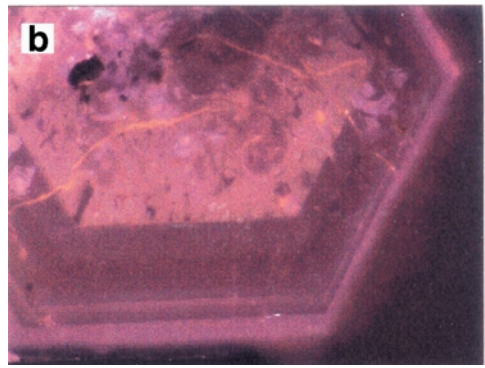
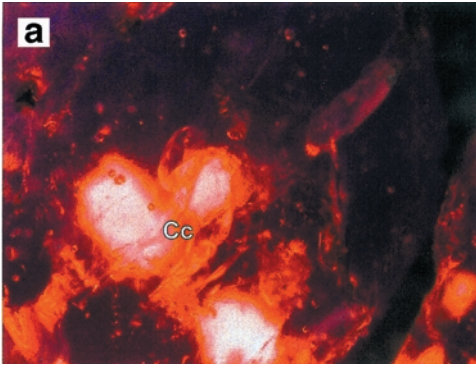
nn: below detection limit in all samples

Chambers, 1996; Rae *et al.*, 1996). Further examples of apatite grains from Mushugai and Svensken (Fig. 2*b,c*) demonstrate that blue to lilac CL is a general feature of apatite from alkaline rocks. The Svensken apatite reveals primary growth zoning not visible under conventional optical microscopy.

The CL emission spectra of the apatite samples from Kovdor, Mushugai and Svensken are dominated by REE-activated luminescence (Figs 3–5). Blue CL is related to Eu^{2+} emission (around 410–430 nm, *cf.* Mariano, 1988). The lilac tint is caused by CL activation due to Ce^{3+} (in the near UV around 360 nm) and Sm^{3+} centres luminescing in the orange to red at 600 and 645 nm (note that the spectra are not corrected for detector response so that emission in the range

from 300 to 450 nm appears to be suppressed). Additional lines are assigned to Dy^{3+} (480 and 570 nm) and Nd^{3+} (in the IR at 870 to 900 nm). The Svensken and Mushugai samples show a pronounced Nd^{3+} emission. However, this feature does not contribute to the visible CL.

In general, CL behaviour of investigated apatite is in accordance with the trace element characteristics of the samples. As a rule, a strong enrichment of the light REE (LREE) including Ce, Nd, Sm and Eu, acting as emission centres in CL, can be found in apatite from alkaline magmatic complexes (see Table 2 and Fig. 6 as well as Landa *et al.*, 1983 for Kovdor apatite; *cf.* Vasil'eva *et al.*, 1978 and Kovalenko *et al.*, 1982 for Mushugai apatite). High La, Ce and Nd concentrations of up to several wt.%, were



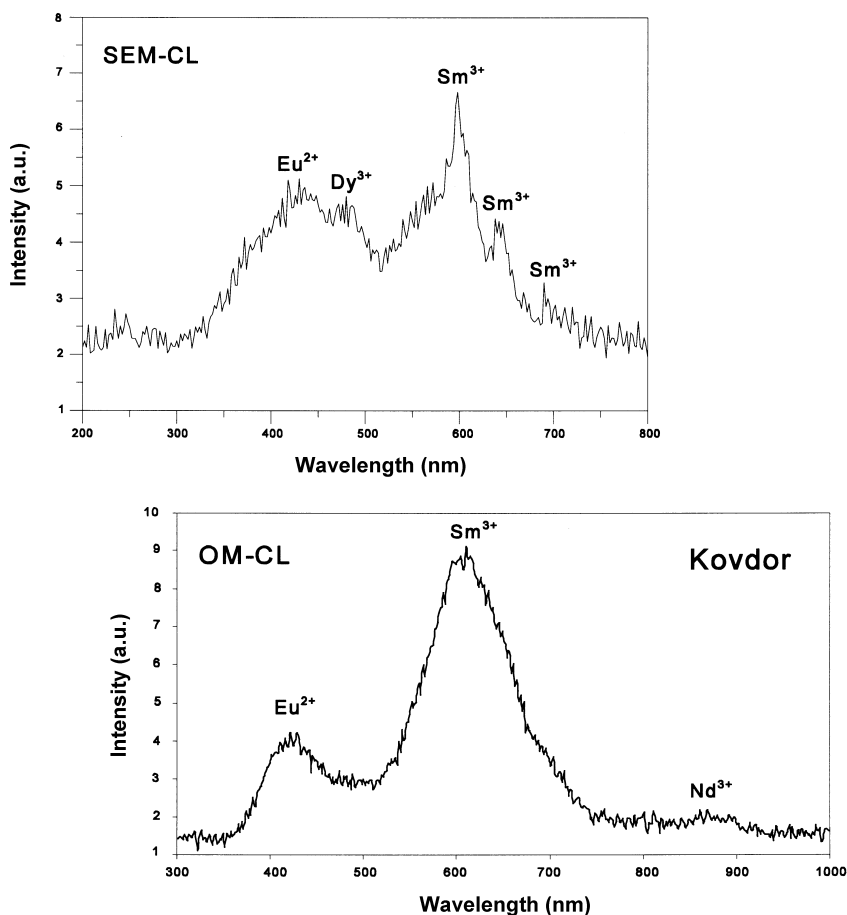


FIG. 3. Cathodoluminescence emission spectra from SEM-CL and OM-CL measurements of the apatite from Kovdor (Kola Peninsula). The spectrum is dominated by emissions due to Eu^{2+} and Sm^{3+} .

detected in the samples from Kovdor, Svensken and Mushugai by microanalysis. This is in accordance with findings for other locations

(Vasil'eva *et al.*, 1978; Rønso, 1989; Rae *et al.*, 1996). Relatively high Na contents found in *LREE*-rich apatite from Kovdor, Mushugai,

FIG. 2 (*opposite page*). Cathodoluminescence micrographs of apatite samples investigated. (a) Blue-violet luminescing apatite grain from a carbonatite of Kovdor (Kola Peninsula) with orange luminescing inclusions of calcite (Cc); (b) violet luminescing apatite grain with oscillatory zoned rim from larvikite of Svensken (Norway); the CL emission is mainly activated by REE^{3+} (*cf.* Fig. 5); (c) apatite crystal from the alkali complex of Mushugai (Mongolia) showing *REE*-activated violet CL (*cf.* CL emission spectrum in Fig. 4); (d) apatite grain from Ermakovka (Transbaikalia); the different growth zones are visible due to sharply contrasting CL activation by $\text{REE}^{2+/3+}$ in the core and Mn^{2+} in the rim, respectively; the rim of the crystal is intergrown with orange luminescing calcite (Cc); the analytical points 1–3 shown in the figure correspond to the spectra in Fig. 8; (e) distinctly zoned apatite grain (A4) from apatite breccia at the granite contact, Ehrenfriedersdorf; the CL emission is activated by Mn^{2+} (*cf.* Fig. 9); (f) apatite from Greifenstein granite, Ehrenfriedersdorf showing both oscillatory and sector zoning (A5); (g) apatite grain (A6) with distinct oscillatory zoning from apatite breccia, Prinzler (Ehrenfriedersdorf); (h) polycrystalline apatite with secondary alteration (A8) from the Sadisdorf tin mine (Germany).

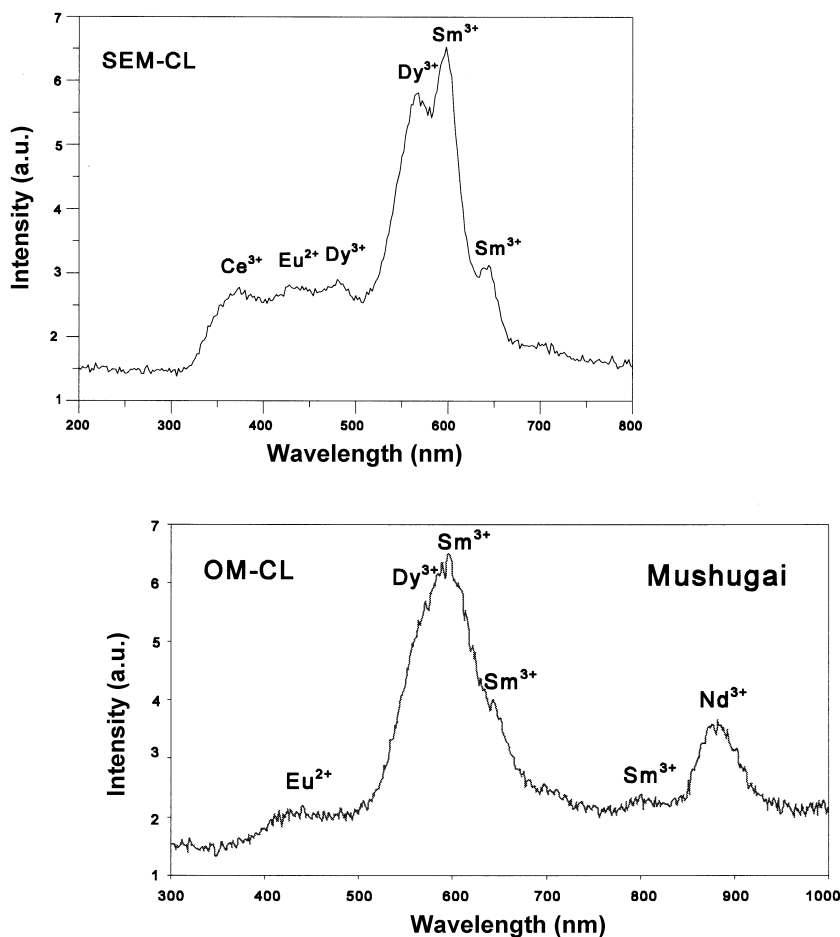


FIG. 4. Cathodoluminescence emission spectra from SEM-CL and OM-CL measurements of apatite from Mushugai Khudug, Mongolia (*cf.* Fig. 2c). The spectra are dominated by strong $REE^{2+/3+}$ -activated luminescence with pronounced Nd^{3+} emission.

Svensken and Ermakovka by ICP-MS (Table 2) and EDX (up to 1.0 wt.% Na_2O) indicate that Na compensation is one important mechanism for charge balancing according to the scheme $2Ca^{2+} \leftrightarrow Na^+ + REE^{3+}$ (Rønso, 1989). Strong enrichment of *LREE*, particularly of La and Ce, is in accordance with the *REE* distribution patterns of the host rocks (*cf.* Kempe and Dandar, 1995). At the same time, the Mn content in apatite is relatively low and ranges from 10 to several 100 ppm (Table 2; Vasil'eva *et al.*, 1978). These values are within the minimum concentration level of Mn detectable as Mn^{2+} by CL spectroscopy in Mn-doped synthetic apatite (Filippelli and Delaney, 1993). Another typical

characteristic of the apatite from alkaline rocks is a high to very high Sr content (up to several wt.%; Landa *et al.*, 1983; Rae *et al.*, 1996). This is confirmed by our observations (0.7 up to 3.6 wt.% SrO detected by EDX, *cf.* also ICP-MS data in Table 2). Moreover, we found that fluorite from such an environment is also strongly enriched in Sr (e.g. Kempe *et al.*, 1999). In accordance with other authors, we can find no correlation between the Sr content and the CL properties of the apatite.

Ermakovka apatite

The core and the rim of the Ermakovka apatite crystals exhibit quite different CL behaviour. The yellowish-green coloured core exhibits blue to

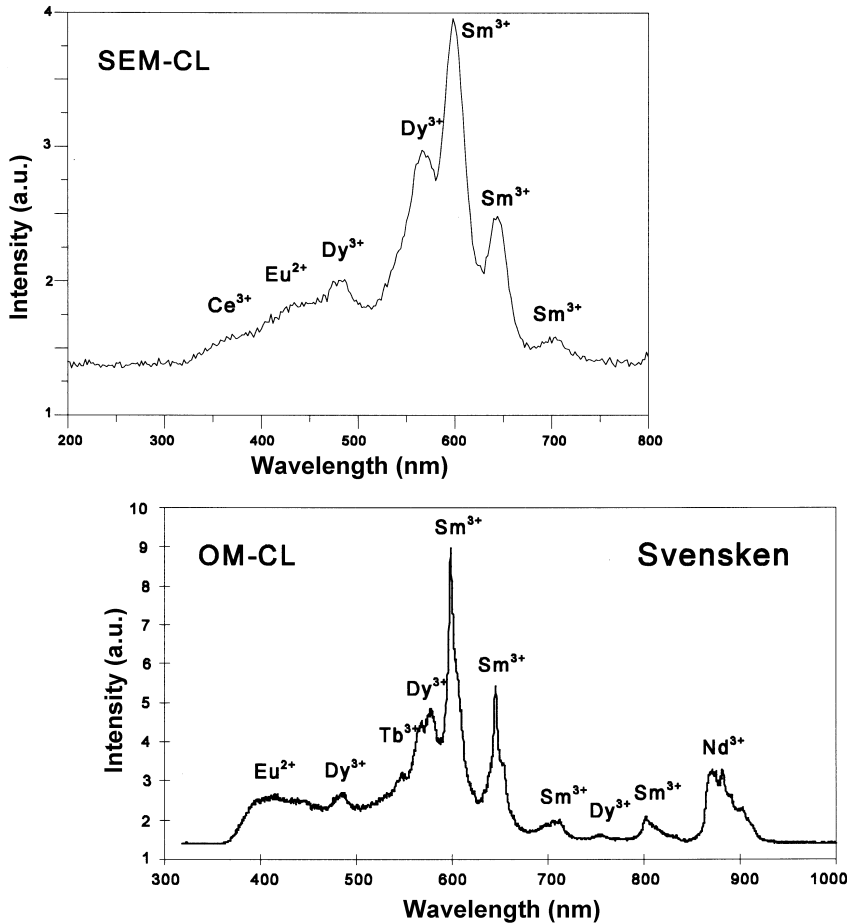


Fig. 5. Cathodoluminescence emission spectra from SEM-CL and OM-CL measurements of the apatite from Svensken, Norway (*cf.* Fig. 2*b*) showing distinct emission lines and bands of Ce^{3+} , Eu^{2+} , Dy^{3+} , Sm^{3+} and Nd^{3+} , respectively.

bluish-violet CL similar to apatite samples from alkaline rock complexes described above. The CL microscopy as well as BSE imaging reveal irregular internal structures due to polycrystalline growth with oscillatory growth zoning (Fig. 2*d* and Fig. 7). By contrast, the monocrystalline, bluish-green rim exhibits greenish-yellow CL as found for apatite from Sn-W deposits (see below) with distinct oscillatory growth zoning. It was not possible to take CL micrographs by SEM-CL imaging due to strong phosphorescence from the rim of the apatite grain. In our experience, phosphorescence is typical of Mn^{2+} centres in Ca minerals (calcite, fluorite, apatite). At the core-rim boundary and in the rim zone itself, intergrowths with red luminescing calcite are

common. In the outer rim, a zone with extremely weak CL intensity was observed, which forms a bright zone in the BSE image (Fig. 7).

The CL spectra of the differently luminescing zones (spots 1–3 in Fig. 2*d*) reveal a change from mainly Ce^{3+} , Eu^{2+} , Sm^{3+} , Dy^{3+} (and Nd^{3+}) activated blue to lilac CL in the inner crystal core to mainly Mn^{2+} (565 nm) and minor REE^{3+} activated greenish-yellow CL in the outer zone (Fig. 8).

Trace element analysis emphasizes the differences between the core and the rim of the Ermakovka apatite crystals. The yellowish core shows *REE* distribution patterns similar to the Kovdor apatite, whereas the bluish-green rim is depleted in *REE* and strongly enriched in heavy

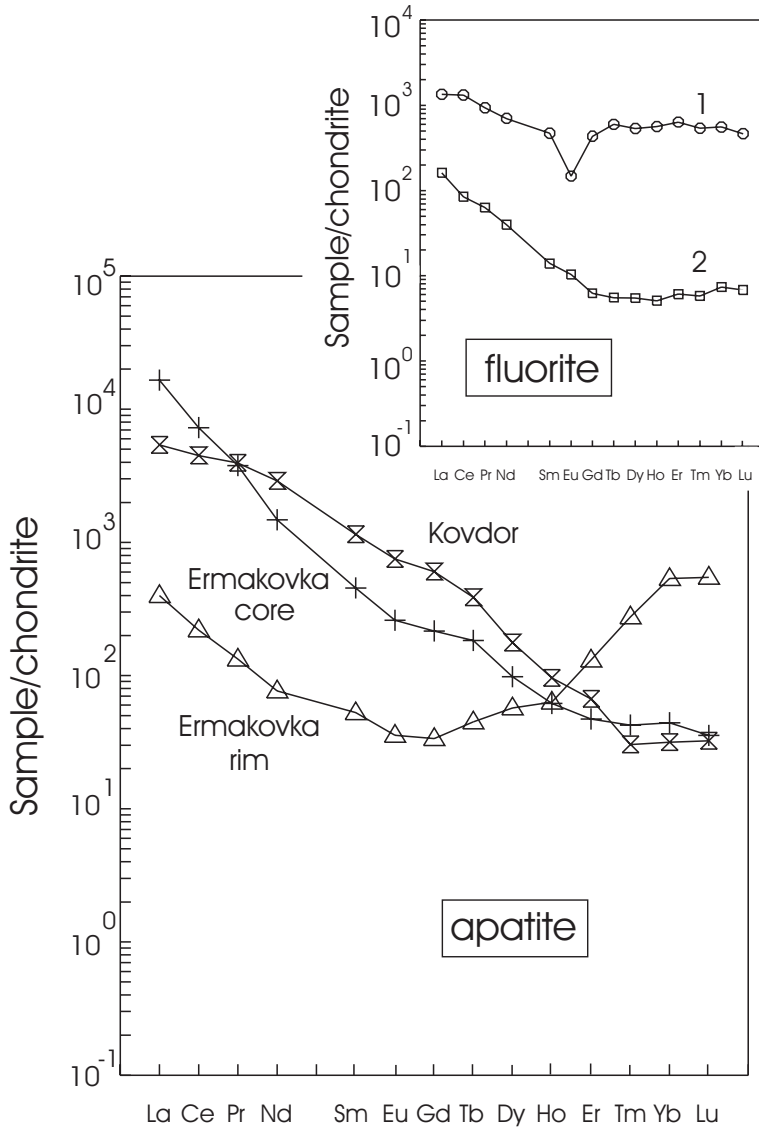


FIG. 6. Chondrite-normalized REE distribution patterns of apatite from Kovdor (Kola Peninsula) and differently coloured rim and core zones of the apatite from Ermakovka (Transbaikalia). The REE distribution patterns (1) of fluorite from a pegmatite in the alkaline granite and (2) of fluorite from the first Ermakovka Be-F ore body (inset) are shown for comparison. Data for fluorite from Kempe and Plötze (unpublished).

REE (HREE) as well as in Y (Fig. 6 and Table 2). The Y/Ho ratio of the rim (169) clearly exceeds the values of the CHARAC box defined by Bau (1996) and the values for the core (14) and the Kovdor apatite (21), which are even below the chondritic value of 28. However, both parts of the crystal are enriched in Sr, the rim (2.9 wt.% Sr) even more than the core (0.8 wt.%). Moreover, as

in the case of Kovdor apatite, Ermakovka apatite is rich in Th (Th 0.04 wt.% in the core and 0.7 wt.% in the rim, with Th>>U).

Variations in luminescence intensities

More detailed microchemical investigation of the core and the rim of the Ermakovka apatite crystals reveals that oscillatory growth zoning

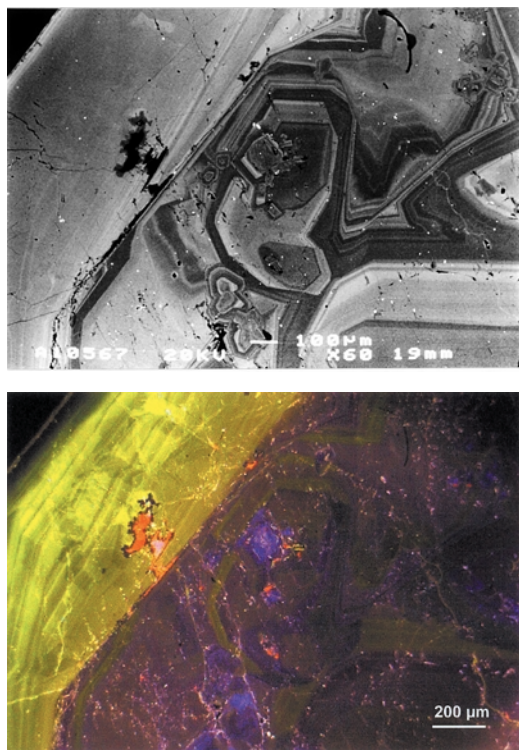


FIG. 7. Comparison of BSE (top) and CL (bottom) micrographs of an apatite crystal from Ermakovka (Transbaikalia). Within the core, the contrast in CL and BSE correlates well with the *REE* content: bright bluish luminescing zones (darker in BSE) are depleted in La and Ce, but enriched in Nd compared to darker luminescing zones (bright in BSE). The rim shows strong yellow Mn^{2+} emission according to strong Mn enrichment (0.3–0.6 wt.% Mn). Oscillatory zoning is only visible by CL. Very high Th content (>0.39 wt.% Th) causes low luminescence efficiency in the outer part of the Mn-rich zone possibly related to strong lattice damage or to charge conversion due to high radioactive irradiation dosages.

visible in CL and BSE images may be related to variations in crystal chemistry. The Sr content is more or less constant in the core (0.65–0.75 wt.% Sr) and in the rim (2.6–2.9 wt.% Sr). Within the core, the contrast in CL and BSE correlates well with the *REE* content: bright luminescing zones (darker in BSE) are depleted in La and Ce, but enriched in Nd compared to darker luminescing zones (bright in BSE). The Mn was below the detection limit of the EDX. The variations in CL intensities may be explained by relative Eu and

Sm enrichment in the Nd-rich zones with related enhanced luminescence intensities. Otherwise, luminescence quenching due to higher concentrations of non-luminescent La centres in the La- and Ce-rich zones may also lead to decreasing integral CL intensities.

The Mn is strongly enriched in the rim (0.3–0.6 wt.% Mn). Accordingly, the rim shows strong Mn^{2+} emission. However, the highest Mn content (1.8 wt.% Mn) was found in the weak luminescing zone. It may be possible to relate the high average Mn content (1.4 wt.%) found by ICP-MS for the whole rim area to this zone. Another characteristic feature of this zone is the very high Th content (>0.39 wt.%). This fact may explain low luminescence efficiency in the Mn-rich zone possibly related to strong lattice damage or to charge conversion due to high radioactive irradiation dosages.

Comparison of CL emission spectra of the apatites from Ermakovka (cores) and Kovdor reveals that both spectra are dominated by Sm^{3+} , Dy^{3+} and Eu^{2+} but the sample from Kovdor shows only very slight Ce^{3+} - and Nd^{3+} -activated CL emission in contrast to the core of the Ermakovka sample. This is remarkable insofar as the *REE* distribution patterns and the concentrations of Ce and Nd in the two apatite samples are very close to each other. Accordingly, the occurrence or absence and the relative intensity of a specific *REE* emission peak in the CL spectrum of apatite cannot be used for quantitative estimations of the relative abundance of these *REE*. Results recently published by Barbarand and Pagel (2001) suggest that there is no simple correlation between contents of the individual *REE* and the emission intensities of the related centres. Mitchell *et al.* (1997) found that the CL spectra of natural apatite result from a subtle interplay of at least three factors: the relative concentration of the individual *REE*, its relative efficiency in activating luminescence and the presence or absence of elements that may act as sensitizers or quenchers. Furthermore, differences in CL behaviour can also be caused by the crystallographic orientation of apatite in thin sections (Murray and Oreskes, 1997; Barbarand and Pagel, 2001) and by charge conversion due to radioactive irradiation. In the case of the apatite samples from Ermakovka and Kovdor, the different contents of Mn, which probably act as a sensitizer of *REE*-activated CL emission (Portnov and Gorobets, 1969; Marfunin, 1979), yield a possible explanation for the variability in luminescence behaviour.

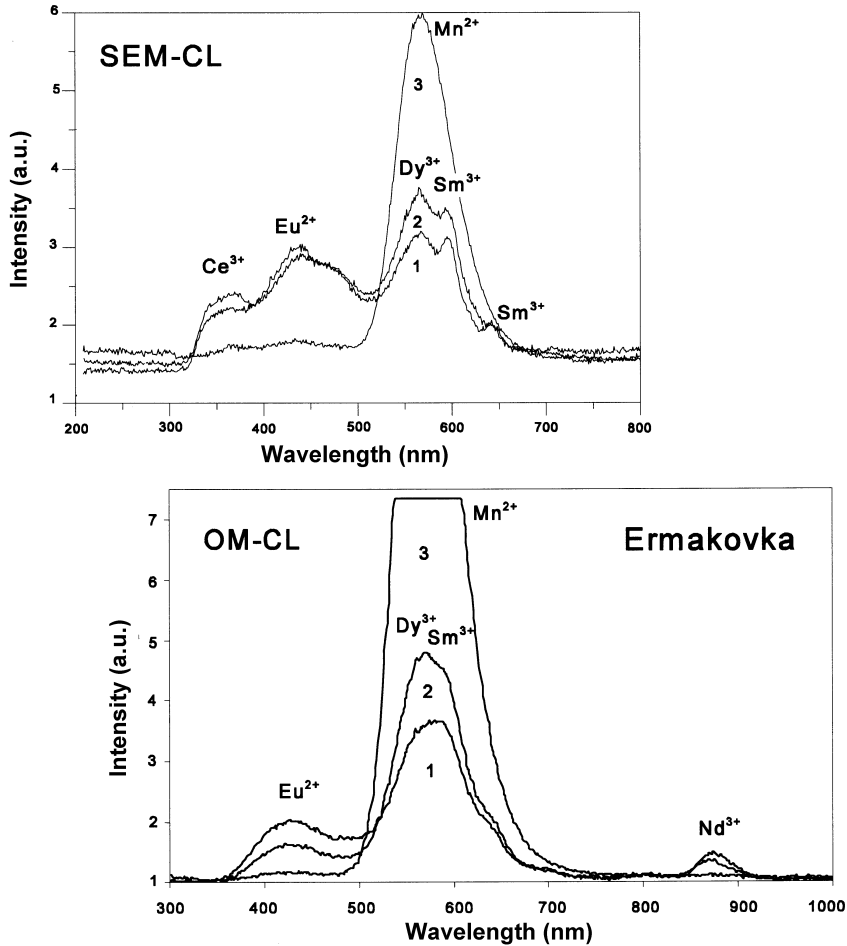


FIG. 8. The CL emission spectra from SEM-CL and OM-CL measurements of the apatite crystal core (1, 2) and rim (3) from the sample from Ermakovka (Transbaikalia). The points analysed are shown in Fig. 2d. The spectra in the core are dominated by $REE^{2+/3+}$ (Ce^{3+} , Eu^{2+} , Dy^{3+} , Sm^{3+} and Nd^{3+})-activated luminescence emission, whereas in the spectrum from the rim, only Mn^{2+} emission is observed.

Apatite in altered granitic rocks from Sn-W deposits

Apatite from the Ehrenfriedersdorf, Sadisdorf and Krasno Sn deposits shows yellowish-green CL independent of the geological environment (granite, greisen, pegmatite, breccia or ore vein). Cathodoluminescence microscopy of the Ehrenfriedersdorf samples reveals internal structures of the single apatite grains, which are not discernible by polarizing microscopy. In most of the investigated samples, distinct oscillatory growth zoning is visible and several grains show additional sector zoning (Fig. 2e–h). Similar internal structures and CL colours were also

reported for apatite crystals from the Panasqueira W-Sn deposit, Portugal (Knutson *et al.*, 1985) and found for apatite from greisenized granite from Vysoky Kamen during our study. The internal structure of the Sadisdorf apatite is more complicated, showing primary growth zoning as well as patchy regions of secondary alteration (Fig. 2h).

As in the Ermakovka sample, it was not possible to image internal structures in Ehrenfriedersdorf samples by SEM-CL due to the strong phosphorescence. By contrast, the defocused electron beam of the CL microscope

produces excellent CL micrographs of the Mn^{2+} -activated apatite luminescence.

Spectral analysis of the CL emission shows only one intensive band centred at 565 nm (2.19 eV, MHW 70 nm) assigned to the emission of Mn^{2+} centres (Fig. 9). The CL intensity of the 565 nm emission band decreases strongly with time. Saturation was reached after 1000–1200 s. In contrast, the emission of the REE^{3+} centres shows stable intensities under electron irradiation. A possible explanation of the emission behaviour of Mn^{2+} is a process of thermoluminescence decay or a decay of sensitizing centres. Intensity decrease of Mn^{2+} -activated luminescence in apatite under the condition of a focused electron beam in a SEM was investigated by Barbarand and Pagel (2001).

The luminescence behaviour of apatite from Sn-W deposits is in general agreement with the trace element contents found. The Mn concentrations are enhanced while the *REE* contents (especially of the *LREE*) are generally low, although some of the apatite samples from Ehrenfriedersdorf have *REE* contents of some hundreds of ppm. However, with the exception of sample A9 (apatite breccia) spectral CL measurements did not detect the characteristic *REE* emission peaks. Only in sample A9, was a slight CL emission in the UV at 365 nm detected, which can probably be related to Ce^{3+}

(Blanc *et al.*, 2000). Obviously, the *REE*-activated CL emission is hidden by the dominant Mn^{2+} luminescence.

Applying time-resolved laser-induced spectroscopy it is possible to determine *REE* luminescence, which has been hidden by other strong emission bands. The differentiation of the specific luminescence centres results from the different delay times, which is in the range of nanoseconds for water-organic complexes, microseconds for rare earth elements and milliseconds for transition metal ions (Gaft *et al.*, 1998). Studies of the Ehrenfriedersdorf apatite by time-resolved laser-induced luminescence reveal that in some cases Eu^{2+} and Dy^{3+} activation is present, which was only detectable using different excitation wavelengths and delay times, respectively (Fig. 10). The Dy^{3+} activation correlates with the relatively high *HREE* contents in the samples.

Time-resolved luminescence measurements allow a comparison of Eu^{2+} emission (*f-d* transition) from all apatite samples investigated. The band position (λ_{max}) shifts from 410 nm in the apatite from Kovdor to 445 nm in the Ehrenfriedersdorf apatite (Fig. 11). Blanc *et al.* (1996) reported a variable position of the Eu^{2+} -activated CL emission band in apatite depending upon the type and composition of the apatite (hydroxy-, chlor- or fluorapatite). However, our results are not in full agreement with their

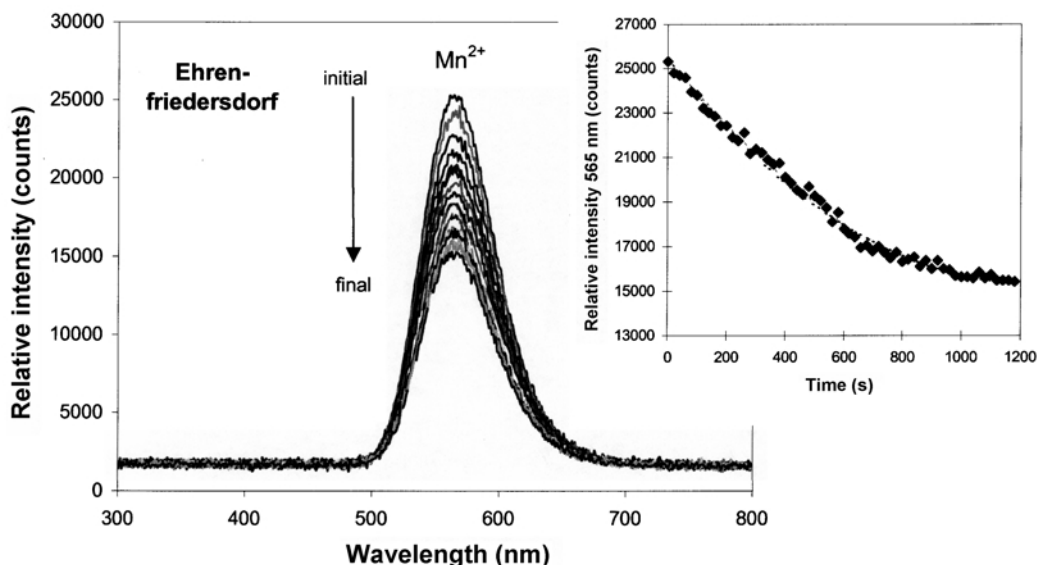


FIG. 9. Time-resolved CL measurements (OM-CL) of the Mn^{2+} emission in an apatite sample (A9) from Ehrenfriedersdorf (Germany). The CL intensity decreases with time reaching apparent saturation after ~ 1200 s.

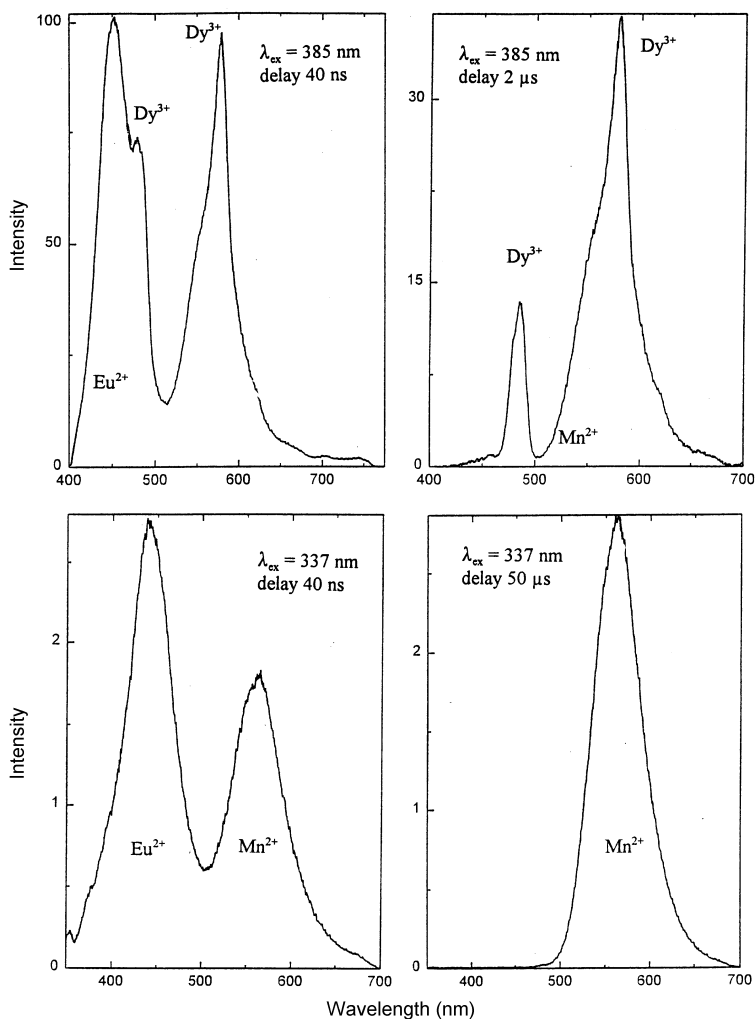


FIG. 10. Influence of excitation energy and delay time on laser-induced luminescence emission spectra (sample A6, Ehrenfriedersdorf, Germany). Besides Mn^{2+} emission, bands related to Eu^{2+} and Dy^{3+} may be detected.

findings, although the trend is the same as predicted (Kovdor apatite is low-F, Ehrenfriedersdorf apatite F-rich and Ermakovka has an intermediate position). Additional investigation is required to resolve the dependence of Eu^{2+} emission on the crystal chemistry of apatite.

Although undetectable by conventional CL spectroscopy, chemically determined REE contents in the apatite samples show a clear correlation with their geological environment (Fig. 12). As we found for fluorite samples from Ehrenfriedersdorf and other Sn deposits (Goldstein *et al.*, 1995; Kempe and Goldstein,

1997, *cf.* Fig. 12), Eu anomalies in the apatite from Ehrenfriedersdorf change from strongly negative to positive from the endo- to the exocontact of the granite. Similar results were also reported by Raimbault (1988) for apatite from Sn-W deposits in the Massif Central (France). Interestingly, all samples investigated by Knutson *et al.* (1985) from the Panasqueira W deposit (Portugal) derived from exocontact ore veins and show distinct positive Eu anomalies. As in the case of fluorite, the variability of Eu contents in apatite may be explained either by differences in incorporation of Eu^{2+} and Eu^{3+}

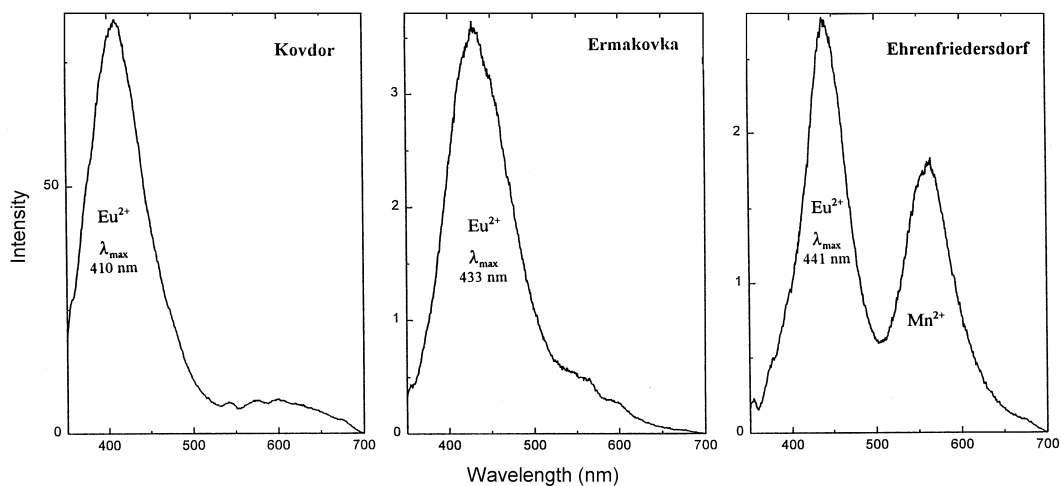


FIG. 11. Shift of the Eu^{2+} emission band from 410 nm (Kovdor apatite) to 441 nm (Ehrenfriedersdorf sample) as detected by laser-induced luminescence spectroscopy.

during rapid changes in the redox conditions or by phase separation processes.

The REE distribution pattern of apatite from an endocontact pegmatite investigated by Trinkler and Martin (1998) shows a distinct tetrad effect (i.e. a split of chondrite-normalized REE patterns into four rounded segments). The enrichment of the HREE leads to very similar REE distribution patterns as for the enclosing granite (Seltmann *et al.*, 1995; Kempe *et al.*, unpubl. data). Inside of the pipe-like topaz-albite granite bodies near the contact with host rocks, the Eu anomaly disappears and REEs are generally depleted, but the tetrad effect and HREE enrichment are still significant (see apatite A5, and fluorite (1) in Fig. 12). In the near exocontact, the HREEs are strongly enriched, while the tetrad effect is weak. Low LREE contents may be interpreted as indicative of only slight admixing of crustal material to the mineral-forming fluid (*cf.* Seifert and Kempe, 1994; Gavrilenko *et al.*, 1997). Both apatite and fluorite show distinct positive Eu anomalies. Interestingly, all of the apatite samples analysed are Sr-rich with the exception of the unaltered pegmatite sample, while fluorite is generally found to be low in Sr.

Luminescence quenching by Fe^{2+} (?)

Variations in luminescence intensity between different growth zones in apatite from Ehrenfriedersdorf can be related to changes in the intensity of the Mn^{2+} emission band (Fig. 13).

Mn^{2+} luminescence in apatite is well known and Mariano (1988) found that low concentrations of Mn (~100 ppm) can serve as an activator for visible CL in apatite. Filipelli and Delaney (1993) reported that synthetic samples with <40 ppm Mn can be considered non-luminescent, based on visual criteria.

Microanalyses perpendicular to the visible CL zoning were performed on one of the apatite samples from Ehrenfriedersdorf (Fig. 14). Only Mn and Fe were found in significant quantities in addition to Ca, P and F. Although the absolute content of Mn increases from the rim to the core, there is no direct effect on the CL intensity. As can be seen in Fig. 14, there is also no direct correlation between CL intensity and the concentrations of Fe. In contrast, a strong correlation exists between the CL intensity and the Mn/Fe ratio. Zones with the highest Mn/Fe ratios exhibit the brightest CL emission, whereas low Mn/Fe ratios (even in zones with high absolute Mn contents) result in dull or no visible CL. While Mn^{2+} acts as a strong CL activator, Fe^{2+} is known as an effective quencher of luminescence (although it was not possible to prove directly the existence of Fe^{2+} in our samples). Therefore, a quantitative estimation of the Mn concentration in apatite using the intensity of the Mn^{2+} -activated emission band at 565 nm, as it was proposed for calcite (Habermann *et al.*, 2000), is not possible. Our result is in agreement with the findings by Filipelli and Delaney (1993) for synthetic apatite,

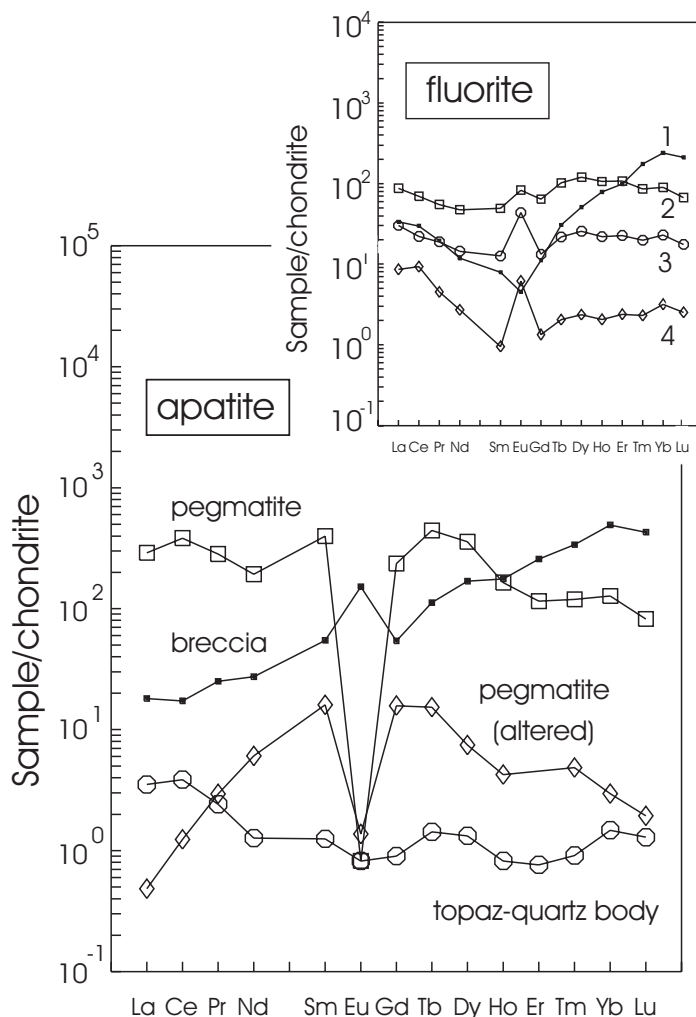


FIG. 12. Chondrite-normalized *REE* distribution patterns of apatite from Ehrenfriedersdorf from different geological environments (pegmatite, topaz-albite granite, apatite-bearing contact breccia). The *REE* content, degree and sign of the Eu anomaly and intensity of the tetrad effect vary in accordance with the sampling site. The *REE* distribution patterns of pale rose fluorite from (1) a greisen veinlet and a succession of green to purple fluorite (2,3,4) from a quartz-cassiterite vein in the exocontact of the Ehrenfriedersdorf granite (inset) are shown for comparison. Data for apatite from pegmatite according to Trinkler and Martin (1998); data for fluorite from Monecke *et al.* (2000b).

although the concentrations of Mn and Fe in our samples are much higher (0.2–0.8 wt.% instead of concentrations <0.2 wt.% for Mn and <0.8 wt.% for Fe)

Concentration quenching of Mn^{2+} luminescence

The apatite from the Vysoky Kamen granite demonstrates another case of luminescence

quenching. The only element detected here by EDX analysis besides Ca, P and F was Mn. There is a clear correlation of the luminescence intensity with the Mn content (Fig. 15). All zones with Mn concentrations $\gg 2.0$ wt.% show dull luminescence, while zones with 1.0–2.0 wt.% Mn luminesce brightly. The effect of luminescence quenching with increasing concentration is known

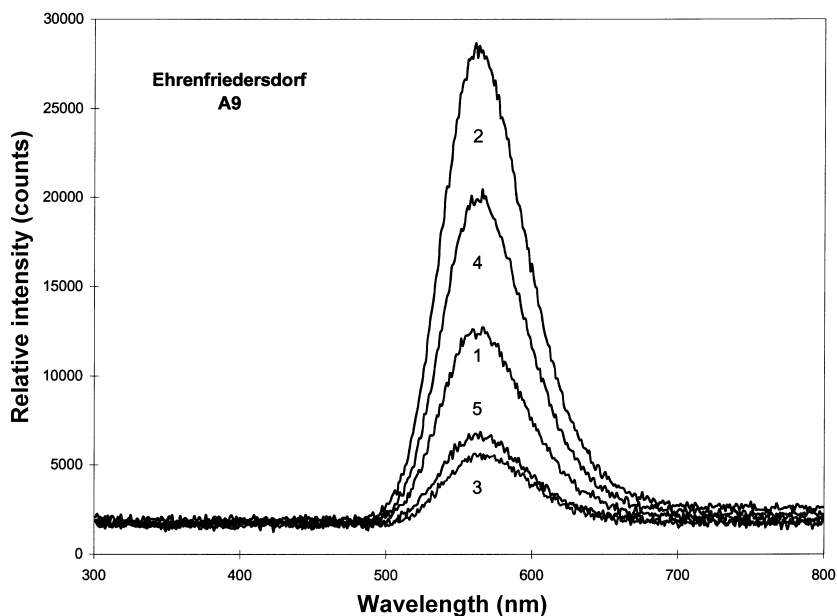


FIG. 13. Variation of Mn^{2+} OM-CL intensity within an oscillatory zoned apatite crystal (A9) from Ehrenfriedersdorf. Measurement points are shown in Fig. 14. The spectra demonstrate that only Mn^{2+} emission is responsible for the signal intensity observed in the OM-CL images of the crystal.

as concentration quenching and was also found, e.g. for *REE* centres in scheelite (Kempe *et al.*, 1991). According to Filipelli and Delaney (1993), Mn^{2+} luminescence intensity saturates at Mn concentrations of ~ 500 ppm.

Complex relations between trace element contents and CL intensities

Although the CL emission of Mn^{2+} and $\text{REE}^{2+/3+}$ is clearly related to Mn and *REE* incorporation in apatite, there is no simple correlation between the contents of these elements and the related emission intensities. Our results suggest possible quenching and sensitizing of *REE*-activated luminescence by La^{3+} and Mn^{2+} centres, respectively.

Likewise, the emission of Mn^{2+} is possibly influenced by charge conversion and lattice damage due to radioactive irradiation. As demonstrated above, in some cases Mn^{2+} -activated CL is quenched by Fe^{2+} and self-quenching mechanisms (high Mn^{2+} content). Additional factors influencing the CL emission intensities in apatite are discussed in the literature (Perseil *et al.*, 2000; Barbarand and Pagel, 2001).

Genetic implications

It can be concluded from our results that there are at least two types of apatite in the two types of mineralization investigated. These may be distinguished easily by their trace element characteristics and CL behaviour.

Apatite from alkaline rocks and carbonatite is typically extremely rich in *LREE* and Sr. In the samples investigated, Th was also found to be prominent. Chemical characteristics are in accordance with the composition of the enclosing rocks and the general CL behaviour. Blue to lilac/violet luminescence may be assigned to high contents of Ce^{3+} , Eu^{2+} and Sm^{3+} emission centres.

Intensive Mn^{2+} emission of apatite from Sn-W deposits is in agreement with general high Mn concentrations and relatively low *REE* concentrations as well as with the *HREE* enrichment.

The *REE* distribution patterns of apatite (as well as of fluorite) from Sn-W deposits may serve as a 'tracer' for *REE* behaviour in such ore systems. These patterns vary in accordance with variations in the geological environment. The high U/Th ratios found in such apatite are also in agreement with the general trend of U enrichment in Sn deposits (Seifert and Kempe, 1994; Morozov *et al.*, 1996).

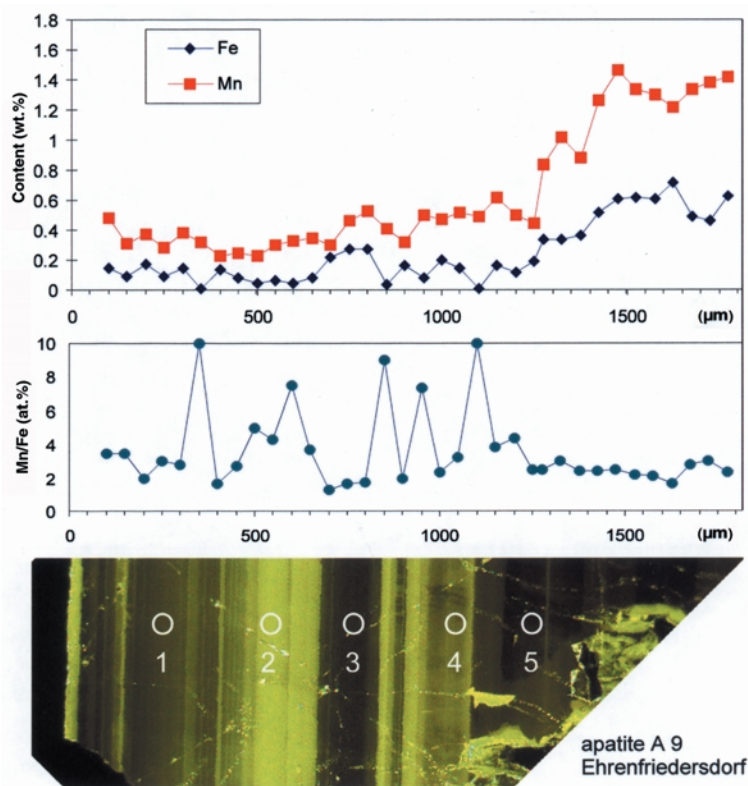


FIG. 14. Correlation between the CL intensity and Mn and Fe contents as well as the Mn/Fe ratio within a profile perpendicular to CL zoning in an apatite crystal (A9) from Ehrenfriedersdorf. Points 1–5 of spectral OM-CL measurements correspond to CL spectra shown in Fig. 13. Luminescence is quenched in zones with low Mn/Fe ratios, whereas high Mn/Fe ratios were detected in bright luminescing zones.

Cathodoluminescence microscopy yields important information on the primary internal growth structures in the apatite pointing to magmatic and hydrothermal formation of the crystals. Nevertheless, secondary metasomatic alteration as in the case of the Sadisdorf sample may also be found. Similar phenomena were described by Coulson and Chambers (1996) for metasomatically altered apatite from the North Qôroq Centre, South Greenland.

The Ermakovka sample provides an interesting case. Here, both types of apatite ('carbonatite' or 'alkaline' type core and 'Sn-W' type rim) may be found in a single crystal. This result confirms our earlier conclusions about the 'mixed' character of Nb-Zr-REE-Be mineralization (Kempe and Dandar, 1995) as well as of the time relations between the earlier 'carbonatite-like' and the later 'Sn-W-like' stages (Kempe *et al.*, 1999). The

Y/Ho ratios of the rim clearly indicate its hydrothermal formation. Similar cases with two types of PL and CL (violet and yellowish) in single apatite crystals were previously described for apatite from altered granitoids of the Mountain Altai/Russia by Nikitina *et al.* (1966) and the Meissen massif, Germany by Wenzel and Ramseyer (1992), respectively.

Conclusions

Cathodoluminescence microscopy reveals internal structures such as growth zoning, alteration, or different generations of apatite. Spectral analysis of the CL emission yields first evidence concerning the distribution of trace elements (in particular rare earth elements and Mn). Moreover, the results of the present investigation show that observed CL colours of apatite and associated CL

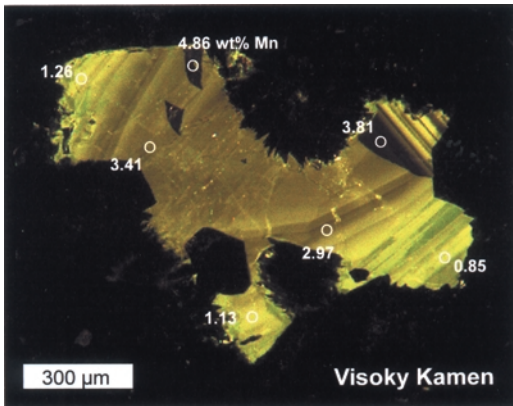


FIG. 15. OM-CL image of an apatite crystal intergrown with quartz and muscovite in the Vysoky Kamen sample (VY 101) demonstrating self-quenching of the Mn^{2+} luminescence. EDX measurement points show that the Mn^{2+} emission intensity is low in zones with very high Mn content.

spectra may reflect specific genetic environments.

The typical blue and lilac/violet CL of apatite from carbonatites is mainly caused by CL activation due to Ce^{3+} , Eu^{2+} and Sm^{3+} . The investigated apatite from a Norwegian larvikite exhibits a similar luminescence behaviour. Apatites from such rocks are enriched in *LREE* and Sr and depleted in Mn. By contrast, the apatite samples from hydrothermal veins with Sn-W mineralization have dominant Mn^{2+} activation causing yellowish CL with distinct oscillatory zoning. This type of apatite has significant lower *REE* contents although the *HREE* are enriched. The *REE* distribution patterns and especially Eu anomalies are sensitive to the geological environment. Samples from the Ehrenfriedersdorf Sn deposit are not only enriched in Mn, but also in U.

As shown for the Ermakovka Be deposit, single apatite crystals may contain both types of apatite – one similar to apatite from carbonatite, the other with properties characteristic of apatite from Sn-W deposits, reflecting the genetic evolution in the deposit.

In general, a simple quantitative correlation between absolute trace element contents and the CL emission intensities does not exist because of certain processes of luminescence sensitizing and quenching. Quenching of Mn^{2+} -activated CL emission by $Fe^{2+(?)}$ as well as concentration quenching were proved for Mn-rich apatite with relatively low *REE* contents. Therefore, detailed

information concerning the principal trace element geochemistry and *REE* distribution patterns can be obtained by direct trace-element analysis only. In consequence, CL investigation and trace element studies are effective only as complementary techniques.

Acknowledgements

The authors would like to thank H. Hildebrandt, W. Klemm, G. Bombach, M. Plötze and P. Dulski for their help in trace element analysis of apatite and fluorite samples. M. Gaft, G. Panczer, D. Wolf and T. Gruner are thanked for the laser-induced luminescence measurements on apatite. U. Kempe is grateful to D. Wolf, S. Dandar, M. Rene and T. Gruner for their assistance with sampling at Mushugai Khudug, Ermakovka, Vysokij Kamen and Ehrenfriedersdorf. The authors are grateful for the helpful comments of two anonymous referees, which helped to improve the manuscript and to S.A.T. Redfern for his editorial efforts.

References

- Barbarand, J. and Pagel, M. (2001) Cathodoluminescence study of apatite crystals. *American Mineralogist*, **86**, 473–484.
- Baskina, V.A., Volchanskaya, I.K., Kovalenko, V.I., Samojlov, V.S., Vladykin, N.V., Goreglad, A.V., Suetenko, O.D. and Shuvalov, V.F. (1978) The potassic alkaline volcanic-plutonic massif at Mushugai Khuduk in Southern Mongolia and related mineralization. *Sovetskaya geologiya*, **4**, 86–99 (in Russian).
- Bau, M. (1996) Controls on the fractionation of isovalent trace elements in magmatic and aqueous systems: evidence from Y/Ho, Zr/Hf, and lanthanide tetrad effect. *Contributions to Mineralogy and Petrology*, **123**, 323–333.
- Blanc, P., Baumer, F., Cesbron, F. and Ohnenstetter, D. (1995) Les activateurs de cathodoluminescence dans des chlorapatites préparées par synthèse hydrothermale. *Comptes Rendus de l'Academie des Science Paris*, **321**, serie IIa, 1119–1126.
- Blanc, P., Panczer, G. and Person, A. (1996) *Example of apatite analysis by cathodoluminescence: teeth of the Mio-Pliocene mastodons*. The French-Israeli workshop on apatites and lasers, Jerusalem, Scientific program and workshop abstracts.
- Blanc, P., Baumer, F., Cesbron, F., Ohnenstetter, D., Panczer, G. and Rémond, G. (2000) Systematic cathodoluminescence spectral analysis of synthetic

- doped minerals: anhydrite, apatite, calcite, fluorite, scheelite and zircon. Pp. 127–160 in: *Cathodoluminescence in Geosciences* (M. Pagel, V. Barbin, P. Blanc and D. Ohnenstetter, editors). Springer Verlag, Berlin, Heidelberg, New York.
- Boudreau, A.E. and Kruger, F.J. (1990) Variation in the composition of apatite through the Merensky cyclic unit in the Western Bushveld Complex. *Economic Geology*, **85**, 737–745.
- Coulson, I.M. and Chambers, A.D. (1996) Patterns of zonation in rare-earth-bearing minerals in nepheline syenites of the North Qôroq Center, South Greenland. *Canadian Mineralogist*, **34**, 1163–1178.
- Elliot, J.C. (1994) *Structure and Chemistry of the Apatites and other Calcium Orthophosphates*. Elsevier, Amsterdam, London, New York, Tokyo.
- Filippelli, G.M. and Delaney, M.L. (1993) The effects of manganese(II) and iron(II) on the cathodoluminescence signal in synthetic apatite. *Journal of Sedimentary Petrology*, **63**, 167–173.
- Finch, A.A. (1992) Cathodoluminescence microscopy in the characterisation of rocks and ceramics. *Proceedings of the Royal Microscopy Society*, **27**, 179–184.
- Finch, A.A. and Fletcher, J.G. (1992) Vitusite – an apatite derivative structure. *Mineralogical Magazine*, **56**, 235–239.
- Fleischer, M. and Altschuler, Z.S. (1986) The lanthanides and yttrium in minerals of the apatite group – an analysis of the available data. *Neues Jahrbuch für Mineralogie Monatshefte*, 1986(10), 467–480.
- Gaft, M., Reisfeld, R., Panczer, G., Blank, P. and Boulon, G. (1998) Laser-induced time-resolved luminescence of minerals. *Spectrochimica Acta Part A*, **54**, 2163–2175.
- Gavrilenko, V., Morozov, M., Kempe, U., Smolenskiy, V. and Wolf, D. (1997) Unusual REE distribution patterns in fluorites from Sn-W deposits of the quartz-cassiterite and quartz-wolframite type. *Journal of the Czech Geological Society*, **42**, 36 (abstract).
- Goldstein, S., Kempe, U. and Klemm, W. (1995) REE in fluorite from tin deposits in the Erzgebirge region: Implications for the origin of Eu-anomalies in Li-F granites. *European Journal of Mineralogy*, **7**, Beiheft 1, 85 (abstract).
- Götze, J., Heimann, R.B., Hildebrandt, H. and Gburek, U. (2001) Microstructural investigation into calcium phosphate biomaterials by spatially resolved cathodoluminescence. *Materialwissenschaft und Werkstofftechnik*, **31**, 1–7.
- Habermann, D., Neuser, R.D. and Richter, D.K. (2000) Quantitative high resolution spectral analysis of Mn²⁺ in sedimentary calcite. Pp. 331–358 in: *Cathodoluminescence in Geosciences* (M. Pagel, V. Barbin, P. Blanc and D. Ohnenstetter, editors). Springer Verlag, Berlin, Heidelberg, New York.
- Hösel, G. (1994) *Das Zinnerz-Lagerstättengebiet Ehrenfriedersdorf/Erzgebirge*. Sächsisches Landesamt für Umwelt und Geologie, Radebeul und Sächsisches Oberbergamt, Freiberg, Germany.
- Hughes, J.M., Cameron, M. and Crowley, K.D. (1991a) Ordering of divalent cations in the apatite structure: crystal structure refinements of natural Mn- and Sr-bearing apatite. *American Mineralogist*, **76**, 1857–1862.
- Hughes, J.M., Cameron, M. and Mariano, A.M. (1991b) Rare-earth-element ordering and structural variations in natural rare-earth-bearing apatite. *American Mineralogist*, **76**, 1165–1173.
- Irber, W. (1999) The lanthanide tetrad effect and its correlation with K/Rb, Eu/Eu*, Sr/Eu, Y/Ho and Zr/Hf of evolving peraluminous granite suites. *Geochimica et Cosmochimica Acta*, **63**, 489–508.
- Jachovsky, T. (1994) Inner structure of tin-tungsten bearing cupolas near Krásno (Slavkovsky Les Mts.). Pp. 137–141 in: *Metallogeny of Collisional Orogens* (R. Seltmann, H. Kämpf and P. Möller, editors). Czech Geological Survey, Prague.
- Kempe, U. and Dandar, S. (1995) Nb-Zr-REE mineralization: a possible source of HREE. Pp. 463–466 in: *Mineral Deposits: from their Origin to their Environmental impacts* (J. Pašavá, T. Kříbek and K. Žák, editors). Balkema, Rotterdam, The Netherlands.
- Kempe, U. and Goldstein, S. (1997) Eu anomalies, tetrad effect and HREE enrichment in fluorites from Sn deposits: evidence for two sources mixing and phase separation. *Journal of the Czech Geological Society*, **42**, 37 (abstract).
- Kempe, U., Trinkler, M. and Wolf, D. (1991) Yttrium und die Seltenerdfofolumineszenz natürlicher Scheelite. *Chemie der Erde*, **51**, 275–289.
- Kempe, U., Götze, J., Dandar, S. and Habermann, D. (1999) Magmatic and metasomatic processes during formation of the Nb-Zr-REE deposits Khaldzan Buregte and Tsakhir (Mongolian Altai): Indications from a combined CL-SEM study. *Mineralogical Magazine*, **63**, 165–177.
- Kharlamov, Yu.S., Kudryavtseva, G.P., Garanin, V.K., Korenova, N.G., Moskalyuk, A.A., Sandomirskaya, S.M. and Shugurova, N.A. (1981) Origin of carbonatites of the Kovdor deposit. *International Geology Review*, **23**, 865–880.
- Knutson, C., Peacor, D.R. and Kelly, W.C. (1985) Luminescence, color and fission track zoning in apatite crystals of the Panasqueira tin-tungsten deposit, Beira-Baixa, Portugal. *American Mineralogist*, **70**, 829–837.
- Kovalenko, V.I., Antipin, V.S., Vladykin, N.V., Smirnova, E.V. and Balashov, Yu.A. (1982) REE distribution coefficients for apatite and REE

- behaviour in magmatic environment. *Geokhimiya*, **2**, 230–243 (in Russian).
- Kuznecov, G.V. and Tarashchan, A.N. (1975) Emission centres in natural apatite. *Konstituciya i svojstva mineralov*, **9**, 120–124 (in Russian).
- Landa, E.A., Krasnova, N.I., Tarnovskaya, A.N. and Shergina, Yu.P. (1983) Distribution of rare earths and yttrium in apatite from ultrabasic and carbonatite intrusions and the origin of apatite mineralization. *Geochemistry International*, **20**, 77–87.
- Lykhin, D.A., Kosticyn, Yu.A.; Kovalenko, V.I., Yarmolyuk, V.V., Sal'nikova, E.B., Kotov, A.B., Kovach, V.P. and Ripp, G.S. (2001) Ore-forming magmatism of the Ermakovka Be deposit in Western Transbaikalia: age, source of magma and relation to mineralisation. *Geologiya rudnykh mestorozhdenij*, **43**, 52–70 (in Russian).
- Marfunin, A.S. (1979) *Spectroscopy, Luminescence and Radiation Centers in Minerals*. Springer-Verlag, Berlin.
- Mariano, A.N. (1988) Some further geological applications of cathodoluminescence. Pp. 94–123 in: *Cathodoluminescence of Geological Materials* (D.J. Marshall, editor). Unwin Hyman, Boston, USA.
- Mitchell, R.H., Xiong, J., Mariano, A.N. and Fleet, M.E. (1997) Rare-earth-element-activated cathodoluminescence in apatite. *Canadian Mineralogist*, **35**, 979–998.
- Monecke, T., Bombach, G., Klemm, W., Kempe, U., Götz, J. and Wolf, D. (2000a) Determination of trace elements in the quartz reference material UNS-SpS and in natural quartz samples by ICP-MS. *Geostandards Newsletter*, **24**, 73–81.
- Monecke, T., Monecke, J., Mönch, W. and Kempe, U. (2000b) Mathematical analysis of rare earth element patterns of fluorites from the Ehrenfriedersdorf tin deposit, Germany: evidence for a hydrothermal mixing process of lanthanides from two different sources. *Mineralogy and Petrology*, **70**, 235–256.
- Morozov, A.M., Morozova, L.G., Trefimov, A.K. and Feofilov, P.P. (1970) Spectral and luminescent characteristics of fluoroapatite single crystals activated by rare earth ions. *Optika i Spektroskopija*, **29**, 590–596 (in Russian).
- Morozov, M., Trinkler, M., Plötze, M. and Kempe, U. (1996) Spectroscopic studies on fluorite from Li-F and alkaline granitic systems in Central Kazakhstan. Pp. 359–369 in: *Granite-related Ore Deposits of Central Kazakhstan and Adjacent Areas* (V. Shatov, R. Seltmann, A. Kremenetsky, B. Lehmann, V. Popov, and P. Ermolov, editors). Glagol Publishing House, St. Petersburg, Russia.
- Murray, J.R. and Oreskes, N. (1997) Uses and limitations of cathodoluminescence in the study of apatite paragenesis. *Economic Geology*, **92**, 368–376.
- Nikitina, E.I., Sotnikov, V.I. and Shcherbakova, M.Y. (1966) Luminescing apatites from granites and greisens of the Mountain Altai. *Zapiski Vsesoyuznogo Mineralogicheskogo Obshchestva*, **95**, 589–593 (in Russian).
- Novikova, M.I., Shpanov, E.P. and Kupriyanova, I.I. (1994) Petrography of the Ermakovskoe beryllium ore deposit, Western Transbaikal region. *Petrology*, **2**, 98–109.
- Ontoev, D.O., Luvsandanzan, B. and Gundsambuu, Ts. (1979) Geology and primary mineralisation of the Mushugai F-REE deposit (Mongolia). *Geologiya Rudnykh Mestorozhdenij*, **3**, 27–42 (in Russian).
- Pan, Y. and Fleet, M.E. (1996) Rare earth element mobility during prograde granulite facies metamorphism: significance of fluorine. *Contributions to Mineralogy and Petrology*, **123**, 251–262.
- Perseil, E.-A., Blanc, P. and Ohnenstetter, D. (2000) As-bearing fluorapatite in manganeseiferous deposits from St. Marcel-Praborna, Val D'Aosta, Italy. *Canadian Mineralogist*, **38**, 101–117.
- Portnov, A.M. and Gorobets, B.S. (1969) Luminescence of apatite from different rock types. *Doklady Akademia Nauk SSSR*, **184**, 110–115 (in Russian).
- Rae, D.A., Coulson, I.M. and Chambers, A.D. (1996) Metasomatism in the North Qôroq centre, South Greenland: apatite chemistry and rare-earth element transport. *Mineralogical Magazine*, **60**, 207–220.
- Raimbault, L. (1988) The recording of fluid phases through REE contents in hydrothermal minerals. A case study: apatites from the Meymac tungsten district (French Massif Central). Pp. 151–159 in: *Mineral Deposits within the European Community* (J. Boissonnas and P. Omenetto, editors). Springer, Berlin, Heidelberg.
- Rakovan, J. and Reeder, R. (1996) Intracrystalline rare earth element distributions in apatite: Surface structural influences on incorporation during growth. *Geochimica et Cosmochimica Acta*, **60**, 4435–4445.
- René, M. (1998) Development of topaz-bearing granites of the Krundum massif (Karlovy Vary pluton). *Acta Universitatis Carolinae*, **42**, 103–109.
- Rieser, U., Krbetschek, M.R. and Stolz, W. (1994) CCD-camera based high sensitivity TL/OSL-spectrometer. *Radiation Measurement*, **23**, 523–528.
- Roeder, P.L., MacArthur, D., Ma, X.-P., Palmer, G.R. and Mariano, A.N. (1987) Cathodoluminescence and microprobe study of rare-earth elements in apatite. *American Mineralogist*, **72**, 801–811.
- Rønso, J.G. (1989) Coupled substitution involving REEs and Na and Si in alkaline rocks from the Ilimaussaq intrusion, South Greenland and the petrological implications. *American Mineralogist*, **74**, 896–901.
- Rundqvist, I.K., Baskina, V.A. and Ontoev, D.O. (1995) Mushugay-Khuduk REE-Fe-F deposit in Southern

- Mongolia. *Global Tectonics and Metallogeny*, **5**, 41–51.
- Seifert, Th. and Kempe, U. (1994) Sn-W-Lagerstätten und spätvariszische Magmatite des Erzgebirges. *European Journal of Mineralogy*, **6**, Beiheft 2, 125–172.
- Seifert, W., Kämpf, H. and Wasternack, J. (2000) Compositional variations in apatite, phlogopite and other accessory minerals of the ultramafic Delitzsch complex, Germany: implications for cooling history of carbonatites. *Lithos*, **53**, 81–100.
- Seltmann, R., Schneider, Th. and Lehmann, B. (1995) The rare-metal granite-pegmatite system of Ehrenfriedersdorf/Erzgebirge: Fractionation and magmatic-hydrothermal transition processes. Pp. 521–524 in: *Mineral Deposits: from their Origin to their Environmental Impacts* (J. Paavá, B. Kõibek and K. Žák, editors). Balkema, Rotterdam, The Netherlands.
- Trinkler, M. and Martin, M. (1998) Zur Mineralogie und Genese des "Stockscheiders" von Ehrenfriedersdorf. *Zeitschrift für geologische Wissenschaften*, **26**, 293–314.
- Vasil'eva, Z.V., Volchanskaya, I.K., Ontoev, D.O., Borisovskij, S.E., and Yakovlevskaya, T.Ya. (1978) On REE-rich zoned apatite from Southern Mongolia. *Izvestiya AN SSSR, ser. geol.*, **2**, 143–148 (in Russian).
- Wenzel, T. and Ramseyer, K. (1992) Mineralogical and mineral-chemical changes in a fractionation-dominated diorite-monzodiorite-monzonite sequence: evidence from cathodoluminescence. *European Journal of Mineralogy*, **4**, 1391–1399.
- Whitney, P.R. and Olmsted, J.F. (1998) Rare earth element metasomatism in hydrothermal systems: The Willsboro-Lewis wollastonite ores, New York, USA. *Geochimica et Cosmochimica Acta*, **62**, 2965–2977.
- Zhang, S., Wang, L. and Yang, W. (1985) Use of REE analysis in apatite to distinguish petrological and mineralogical series of granitic rocks. *Geochimica*, **1**, 45–57.

[Manuscript received 18 May 2001;
revised 20 November 2001]